Systems & Control Transactions

Original Research Article
Peer Reviewed Conference Proceeding
ESCAPE 36 - European Symposium on Computer Aided Process Engineering
Sheffield, UK. 21-24 June 2026

PSE PRESS

A Process Modeling Approach for Water and Energy Optimization in Geologic Hydrogen Extraction

Caroline Kaitano[a], and Thokozani Majozi[a]*

[a] University of the Witwatersrand, School of Chemical and Metallurgical Engineering, Braamfontein, Gauteng, South Africa
* Corresponding Author: thokozani.majozi@wits.ac.za.

ABSTRACT

Geologic hydrogen has emerged as a promising low-carbon energy vector, but its sustainable recovery requires effective stimulation and production strategies. This study presents an integrated process-modeling framework for evaluating hydrogen extraction from hydraulically stimulated reservoirs. The framework combines fracture propagation, damage evolution, Darcy-scale multiphase flow, permeability–aperture dynamics, and a dual-porosity dual-permeability (DPDP) representation to simulate hydrogen production in fractured source rock systems. In addition to production dynamics, the framework tracks operational water and energy inputs and incorporates a simplified reaction-extent formulation to represent hydrogen generation under data-limited conditions. The model was benchmarked against published shale gas production results to evaluate its ability to reproduce fracture-controlled production behavior and was subsequently applied to a representative multi-well hydrogen development scenario. Simulation results indicate that hydrogen production is strongly fracture-dominated, with fracture pathways accounting for more than 98% of total modeled output. Under the simulated conditions, the system produced approximately 1.13 million kg of hydrogen, with an estimated operational energy intensity of 3.4 MJ/kg H_2 and water consumption of 0.02 m^3/kg H_2. These values represent model-based estimates within the defined operational system boundary and illustrate the potential performance indicators that the framework can generate. Per-well analysis reveals variability in water and energy efficiency across the multi-well system, highlighting the importance of fracture design and reservoir characterization. The simulations also indicate that matrix contributions to total recovery are limited under the assumed conditions, suggesting potential benefits from strategies that enhance matrix reactivity or transport processes. Overall, the framework provides an integrated approach for exploring hydrogen production dynamics together with associated resource requirements. As field and experimental data for geologic hydrogen systems become available, the framework can be further refined through improved parameterization, sensitivity analysis, and calibration to support future technical, environmental, and economic assessments.

Keywords: Geologic hydrogen, Extraction, Modelling and Simulations, Optimization, Energy, Water

INTRODUCTION

The intensifying global energy crisis, propelled by geopolitical instability and the objectives of the 2015 Paris Agreement to restrict warming to below 2 °C and achieve net-zero emissions by 2050, highlights the pressing necessity for a swift transition to reliable, sustainable energy sources [1]. A significant issue in this shift is the identification of carbon-free, economically feasible, and sustainable energy sources [2].

Hydrogen has emerged as a cornerstone of the global energy transition, offering a versatile, low-carbon energy vector capable of decarbonizing hard-to-abate sectors [3, 4]. While manufactured hydrogen from electrolysis or reforming dominates current discourse, these pathways remain constrained by high costs, scalability challenges, and significant energy or carbon footprints [5]. In contrast, geologic hydrogen naturally generated in the subsurface through processes such as serpentinization, radiolysis, and iron oxidation has recently attracted attention as a potentially abundant and low-emission alternative [6]. The accidental discovery and subsequent exploitation of native hydrogen in Bourakébougou, Mali, demonstrated the feasibility of harnessing subsurface hydrogen resources, catalyzing global interest in both natural accumulations and engineered stimulation approaches [6–8].

Recent research has introduced the concept of stimulated geologic hydrogen production, sometimes termed "orange hydrogen, " which seeks to actively engineer subsurface conditions to accelerate hydrogen-generating reactions in iron-rich ultramafic rocks [9, 10]. Techniques such as hydraulic fracturing, thermal treatment, chemical stimulation, and electrical reservoir stimulation have been proposed to enhance permeability, reactive surface area, and geochemical kinetics [11]. Numerical modeling studies indicate that stimulation can increase hydrogen yields by several orders of magnitude compared to unstimulated systems, with fracture networks and damage zones playing a decisive role in enabling efficient hydrogen migration and recovery [11, 12]. However, despite promising laboratory and pilot-scale results, critical uncertainties remain regarding the efficiency, sustainability, and resource requirements of such systems [13].

A key challenge lies in balancing water and energy inputs with hydrogen outputs. Stimulated systems require a continuous water supply to sustain serpentinization, while compression and fracturing impose significant energy costs [14]. Recent circularity studies suggest that integrating waste heat recovery and water recycling can reduce operational burdens, yet quantitative assessments of water–energy–hydrogen balances at the reservoir scale remain scarce. Moreover, while fracture-dominated pathways have been shown to account for the majority of production [15], the contribution of the rock matrix is often minimal, and this raises questions about how stimulation design and reservoir characterization can be optimized.

Against this backdrop, this study introduces an integrated process-modeling framework for evaluating geologic hydrogen recovery in hydraulically stimulated reservoirs. The framework combines fracture propagation, damage evolution, Darcy-scale multiphase flow, permeability–aperture dynamics, and a dual-porosity dual-permeability (DPDP) representation to simulate hydrogen production from fractured source rock systems.

Existing fractured-reservoir models primarily focus on fluid flow and production forecasting, while reactive transport models emphasize geochemical reactions and species transport in porous media. These approaches are typically applied independently and are not specifically designed to evaluate the coupled production dynamics and resource requirements associated with geologic hydrogen extraction.

The framework developed in this study integrates fracture-controlled flow behavior with a simplified representation of hydrogen-generating reactions and explicit accounting of water and energy inputs. This system-level integration enables quantitative evaluation of water–energy–hydrogen trade-offs in hydraulically stimulated reservoirs. It provides a basis for exploring operational constraints and efficiency considerations in geologic hydrogen development.

By linking subsurface production dynamics with resource-use metrics, the framework provides a tool for estimating production performance, evaluating resource consumption requirements, and informing future optimization of stimulation strategies. In the absence of field-scale geologic hydrogen datasets, the framework is intended as a first-order modeling approach that can be refined as new experimental and field observations become available.

The objectives of this study are therefore to (i) develop the integrated modeling framework, (ii) demonstrate its application to hydraulically fractured hydrogen systems, and (iii) evaluate production performance together with associated water and energy requirements.

FRAMEWORK DEVELOPMENT

This study develops an integrated process modelling framework to quantify hydrogen generation, transport, and recovery in hydraulically stimulated geologic hydrogen systems. The approach couples (i) fracture propagation and damage evolution, (ii) dual-porosity dual-permeability (DPDP) fluid flow, (iii) multiphase reactive transport, (iv) permeability-aperture evolution, and (v) thermal feedback from serpentinization reactions.

Governing Equations

In order to simulate the generation and transport of geologic hydrogen in the source rock, mass and energy conservation were solved.

$$\rho C_p \frac{\partial T}{\partial t} + \nabla \cdot \left(\rho_f C_{p,f} \vec{v} T - k \nabla T\right) = q_{rad} + \Delta H_r R_H \quad (1)$$

Where ρ is the rock density, C_p is the rock's specific heat capacity, ρ_f is the fluid density, $C_{p,f}$ is the fluid specific heat capacity, $\vec{v}$ is the fluid velocity (m/s), T is the temperature, k is the thermal conductivity, q_{rad} is the radiogenic heat generation, ΔH_r is the heat from serpentinization (J/mol) and R_H is the generation rate from serpentinization (mol/m^3.s).

$$\frac{\partial C_H}{\partial t} + \nabla \cdot \left(-D_H \nabla C_H + \vec{v} C_H\right) = R_H - R_{microbial} - R_{leak} \quad (2)$$

Where D_H is hydrogen diffusivity, C_H is hydrogen concentration (mol/m^3), $R_{microbial}$ is the microbial hydrogen consumption, and R_{leak} is the loss due to leakage through fractures or faults.

$$R_H = \frac{\varepsilon_{max}}{b} \bullet \frac{exp\,(\frac{-t-t_{1/2}}{b})}{(1+exp\,(\frac{-t-t_{1/2}}{b}))^2} \quad (3)$$

$$\varepsilon(t) = \frac{\varepsilon_{max}}{1+exp(\frac{-t-t_{1/2}}{b})} \quad (4)$$

Where ε_{max} is the maximum reaction extent(%), t is the time in days, $t_{1/2}$ is the time to reach half-reaction extent (days), b is the rate constant in days, and $\varepsilon(t)$ is the reaction extent.

The fracture propagation with damage evolution and the aperture evolution are accounted for using equations (5)-(7).

$$\frac{dD}{dt} = A_d \bullet (\sigma - \sigma_{crit})_+^n \quad (5)$$

Where D is the damage variable, A_d is the rate constant for damage growth, σ is the applied stress, and σ_{crit} is the threshold for damage initiation.

$$k(D) = k_o \bullet (1 + \alpha_k D) \quad (6)$$

$$a(D) = a_o \bullet (\beta D) \quad (7)$$

Where a(D) is the evolving fracture aperture and α_k and β are sensitivity coefficients.

Mass transfer between the fracture and the fracture and matrix is accounted for using the dual permeability model.

$$Q_{f\to m} = \alpha \bullet (P_f - P_m) \quad (8)$$

Where $Q_{f\to m}$ is the flowrate between fracture and matrix (m^3/s), α is the transfer coefficient (s^{-1}), and P_f, P_m is the pressures in fractures and matrix.

The temperature feedback and fluid temperature change in the fractures is accounted for using equations (9) and (10), respectively.

$$Q_{rxn} = \Delta H_r R_H \to T^{n+1} = T^n + \frac{\Delta t}{\rho_r C p_r} Q_{rxn} \quad (9)$$

$$T_{out} = T_g - (T_g - T_{in}) \bullet exp(\frac{-h_c A}{\dot{m} C_{p,f}}) \quad (10)$$

Where T_{out} is the outlet fluid temperature, T_g is the rock matrix temperature, $\dot{m}$ is the fluid mass flowrate (kg/s), A is the contact area (m^2), and h_c is the convective heat transfer coefficient.

Numerical Implementation

The governing equations describing fluid flow, hydrogen transport, and reaction extent were solved numerically using a finite-difference discretization on a structured grid. The spatial domain representing the reservoir and fracture system was discretized into grid blocks that capture both matrix and fracture regions within the dual-porosity dual-permeability framework. Grid resolution was selected to resolve fracture–matrix interactions while maintaining computational efficiency adequately.

Time integration was performed using an implicit time-stepping scheme to ensure numerical stability for the coupled flow, transport, and reaction processes over the simulation period. The time step size was adjusted to capture the early-time production dynamics and longer-term stabilization behavior observed in the system.

All simulations were conducted over a 365-day production period using the parameter set described in Table 1. The computational implementation was developed in a numerical simulation environment capable of solving coupled nonlinear equations representing subsurface flow and reaction processes. Simulation runtimes for the scenarios presented in this study were on the order of minutes on a standard workstation, indicating that the framework is computationally efficient for scenario analysis and preliminary system evaluation.

Table 1: Parameters used in this study

Parameter	Value
Number of wells	5
Initial reservoir pressure	50 MPa
Reservoir thickness	50 m
Rock density	3300 kg/m^3
Rock heat capacity	870 J/kg·K
Rock thermal conductivity	3.45 W/m·K
Matrix porosity	0.02
Matrix permeability	5×10^{-12} mD
Hydrogen viscosity	8.90×10^{-6} Pa·s
Enthalpy of reaction	–520 J/mol
Matrix diffusivity	5×10^{-8} m^2/s
Fracture diffusivity	1×10^{-5} m^2/s
Reaction extent	0.30
Half-life	60 days
Hydrogen heat capacity	14, 300 J/kg·K
Hydrogen density	80 kg/m^3

FRAMEWORK VALIDATION

To evaluate the proposed framework, published shale gas production results were used as a reference dataset for benchmarking. Since direct field-scale data for geologic hydrogen are not yet available, shale gas was selected due to its analogous subsurface extraction processes and reliance on hydraulic fracturing. Parameters from Zhao et al. [16], who developed a variable-fidelity radial basis function (VFRBF) surrogate-assisted model for multi-objective fracture stage placement optimisation, were incorporated into the framework to generate simulated production curves. This allowed the framework outputs to be compared against a well- characterised set of published results. The resulting cumulative production curves for a single well are shown in Figure 1, illustrating the temporal evolution of gas production predicted by the framework. Quantitative performance metrics further confirm the close alignment, with R^2 =0.9928, RMSE=0.2689, and MAE=0.2108. These values indicate that the framework reproduces single-well production dynamics with high fidelity, explaining more than 99% of the variance in the surrogate data while maintaining average errors below 0.3 million m³.

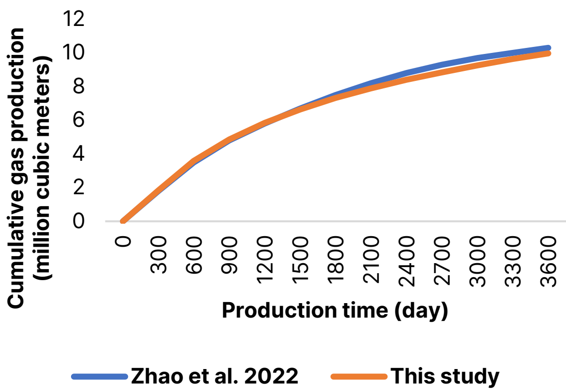

Figure 1. Cumulative production curves for a single well comparing Zhao et al. [16] and this study. The framework demonstrates strong agreement with the VFRBF model, supported by performance metrics: R^2 = 0.9928, RMSE = 0.2689, and MAE = 0.2108.

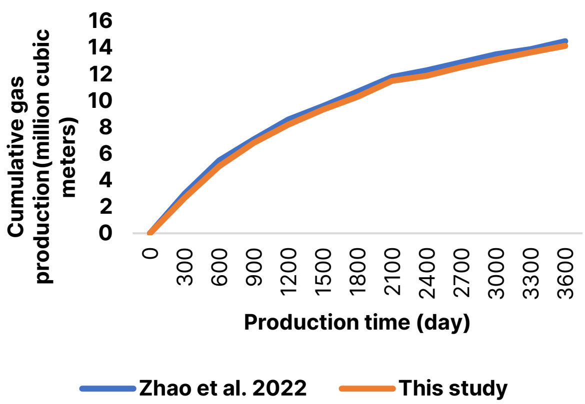

Figure 2. Cumulative production curves for multiple wells comparing Zhao et al. [16] and this study. The outputs from this framework show close alignment with the VFRBF model, validated by performance metrics: R^2 = 0.9940, RMSE = 0.3333, MAE = 0.3154.

The cumulative production curves produced by the framework show strong agreement with the results reported by Zhao et al. [16], suggesting that the framework can reliably capture the dynamics of resource extraction and production decline in hydraulically fractured reservoirs. A multi-well comparison is presented in Figure 2, highlighting consistent trends and close alignment between the aggregated outputs and the results reported by Zhao et al. over the production period. Statistical validation supports this observation, with R^2 =0.9940, RMSE=0.3333, and MAE=0.3154. These metrics show that the framework explains over 99% of the observed variance at the multi-well scale, with deviations representing less than 2% of total cumulative production.

It should be noted that this comparison primarily evaluates the framework's ability to reproduce production decline behavior in hydraulically fractured reservoirs. The benchmarking exercise, therefore, tests the production forecasting component of the framework but does not constitute direct validation of the coupled reactive transport processes, thermal feedback mechanisms, hydrogen generation kinetics, or the water–energy accounting components included in the model. Because field-scale datasets for geologic hydrogen systems are not yet available, validation of these processes remains limited. The present comparison should therefore be interpreted as a model-to-model benchmarking exercise focused on production dynamics, providing an initial consistency check rather than a comprehensive validation of all coupled processes.

While shale gas differs from hydrogen-bearing formations in geochemical properties, the observed alignment supports the framework's validity as a first-order estimation tool. This validation establishes confidence in the framework's applicability and provides a foundation for future refinement once empirical data on geologic hydrogen become available.

FRAMEWORK APPLICATION

Following benchmarking with shale gas data, the framework was applied to geologic hydrogen extraction scenarios to demonstrate its utility in estimating resource usage under realistic subsurface conditions. The application considered hydrogen generation from source rock formations, parameterized with representative geologic and operational inputs. In this case, a multi-well development consisting of five hydraulically fractured wells was assumed, reflecting typical field-scale deployment strategies in unconventional reservoirs. Table 1 shows the parameters used in this study.

The framework integrated source rock properties, fracture design parameters, and well spacing to simulate cumulative hydrogen production and associated resource requirements. The multi-well configuration allowed assessment of inter-well interactions and aggregate production behavior, providing insight into scalability and efficiency. Results indicated that the framework successfully captures the production dynamics across the five-well system, generating a cumulative production curve that highlights both individual well contributions and overall field performance. This application demonstrates the framework's adaptability to geologic hydrogen contexts and establishes a basis for future refinement once empirical hydrogen production data become available.

The reaction extent formulation used in this study is intended as a phenomenological representation of hydrogen generation from subsurface water–rock interactions. Because field-scale kinetic data for geologic hydrogen systems remain limited, the model employs simplified parameters that capture the dominant temporal behavior of reaction-driven resource generation.

In this formulation, the half-life parameter represents an effective kinetic timescale governing the rate at which reactive minerals contribute to hydrogen generation under reservoir conditions. The maximum reaction extent parameter represents the fraction of the reactive mineral inventory that can realistically participate in hydrogen-producing reactions, accounting for constraints such as mineral accessibility, transport limitations, and thermodynamic equilibrium.

These parameters should therefore be interpreted as effective model parameters rather than direct measurements of intrinsic reaction kinetics. Their values were selected to represent plausible reaction timescales reported in studies of water–rock reactions and hydrogen-generating geochemical systems. Because uncertainties remain in these processes, the present formulation is intended as a first-order approximation suitable for framework development. Future work will include systematic sensitivity analysis and calibration as experimental and field data for geologic hydrogen systems become available.

The simulation results reveal a stark contrast between hydrogen production from the matrix and fracture domains. As shown in Figure 3, the fracture system dominates hydrogen output, with production rates rapidly rising to approximately 4000 kg/day within the first 100 days and remaining stable through 365 days. In contrast, matrix production remains negligible throughout the simulation period, indicating a limited contribution to the overall yield. This disparity underscores the critical role of fracture-enhanced transport and reactivity in enabling scalable hydrogen recovery from source rocks. The results demonstrate the framework's sensitivity to diffusivity and permeability parameters and highlight the importance of fracture network design in optimizing hydrogen extraction efficiency.

Figure 4 illustrates the temporal evolution of hydrogen output and water utilization efficiency over a 365-day simulation period. Hydrogen production rate increases steadily during the initial 180 days, reaching a plateau at approximately 4000 kg/day, consistent with fracture-dominated flow behavior observed in earlier results. Simultaneously, water efficiency, defined as kilograms of hydrogen produced per cubic meter of water used, rises gradually and reaches about 57 kg H_2/m^3 by day 365. This trend reflects improving resource utilization over time, as the system becomes more productive without proportional increases in water input.

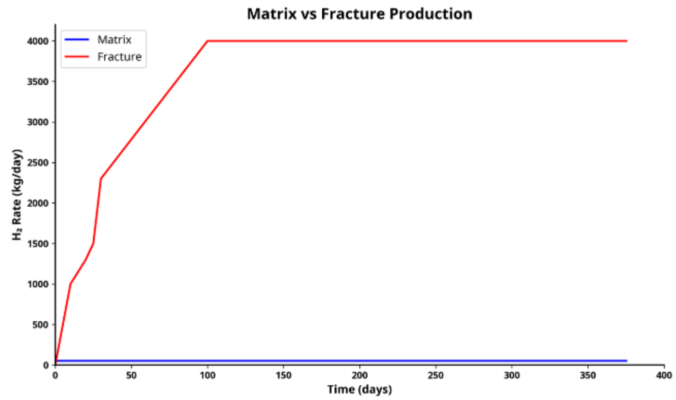

Figure 3. Hydrogen production rate over time from matrix and fracture domains

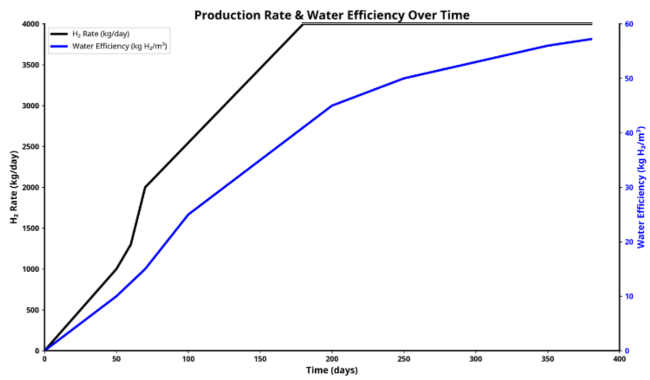

Figure 4. Hydrogen production rate and water efficiency over time

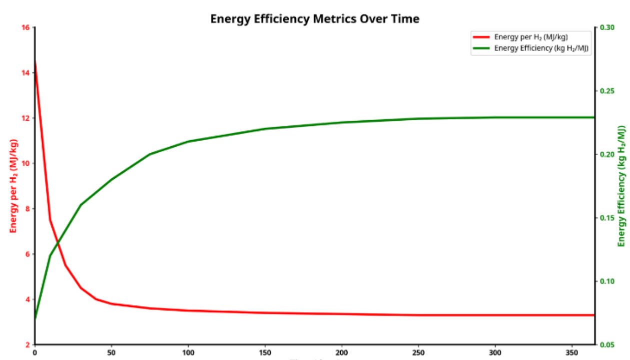

Figure 5. Energy efficiency metrics over time during hydrogen extraction

The energy and water estimates reported in this analysis are defined within a well-field operational system boundary. The accounting includes the primary operational energy inputs associated with subsurface hydrogen extraction, specifically hydraulic fracturing operations, fluid pumping during production, and gas compression required for surface handling of the produced gas stream. Upstream processes such as drilling equipment manufacturing, infrastructure construction, and downstream processes, including hydrogen purification, storage, or long-distance transport, are not included. Consequently, the reported energy and water metrics represent direct operational requirements rather than a full life-cycle assessment. When comparisons are made with conventional hydrogen production pathways, they should therefore be interpreted as contextual benchmarks rather than strict life-cycle comparisons.

The co-evolution of these metrics highlights the framework's ability to capture both production dynamics and sustainability indicators. The plateau in hydrogen rate suggests stable fracture performance, while the continued rise in water efficiency implies that early water investment yields increasingly favorable returns. These insights are critical for evaluating the viability of geologic hydrogen extraction, especially in water-constrained environments. The results reinforce the importance of fracture design and operational timing in optimizing both output and efficiency.

Figure 5 provides insight into the evolving energy performance of the hydrogen extraction system. Over the 365-day simulation, the energy required per kilogram of hydrogen decreases steadily from around 16 MJ/kg to approximately 4 MJ/kg, indicating improved thermodynamic efficiency as the system stabilizes. Concurrently, the energy efficiency, expressed as kilograms of hydrogen produced per megajoule of input energy, increases and plateaus near 0.25 kg H_2/MJ. This inverse relationship reflects the system's optimization over time, where less energy is needed to sustain high hydrogen output. These trends underscore the framework's ability to capture not only production dynamics but also energy sustainability, offering a valuable metric for evaluating the long-term viability of geologic hydrogen operations.

The key performance indicators over the 365-day simulation period provide a comprehensive snapshot of the system's overall efficiency and sustainability. Total hydrogen production reached 1, 132, 287 kg, demonstrating the scalability of the multi-well fracture-based extraction approach. Water consumption averaged 0.02 m^3 per kilogram of hydrogen, translating to an overall water efficiency of 57 kg H_2/m^3. This aligns with the trends observed in the water efficiency graph, confirming that the system maintains high productivity with minimal water input.

Energy consumption averaged 3.40 MJ per kilogram of hydrogen, yielding an overall energy efficiency of 0.29 kg H_2/MJ. These values reflect the system's ability to optimize energy use over time, as previously shown in the declining energy-per-kilogram and rising energy efficiency metrics. Together, these indicators validate the framework's capacity to simulate not only production dynamics but also resource efficiency, offering a robust foundation for evaluating geologic hydrogen extraction under realistic operational constraints.

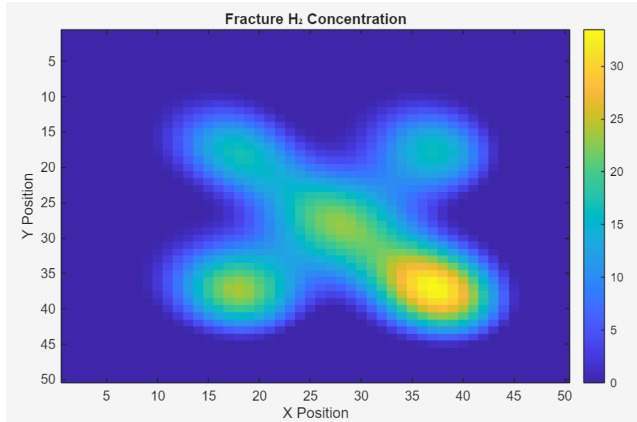

Figure 6. Fracture H_2 concentration distribution

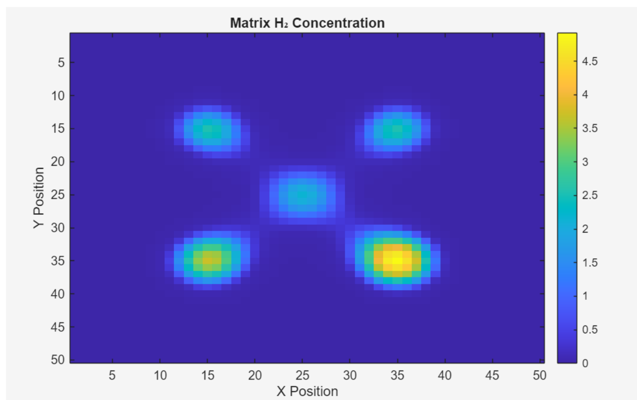

Figure 7. Matrix H_2 concentration distribution

The fracture hydrogen concentration distribution shown in Figure 6 demonstrates the dominant role of fracture networks in controlling recovery efficiency. Concentrations along the fracture plane are relatively uniform and continuous, reflecting the high permeability and aperture evolution captured in the dual-porosity dual-permeability (DPDP) framework. This behavior confirms that fracture-dominated pathways serve as the primary conduits for hydrogen transport, accounting for the vast majority of cumulative production. The spatial spread of hydrogen within the fracture system highlights how fracture propagation and connectivity enable rapid mobilization of hydrogen, minimizing diffusion limitations and ensuring efficient recovery at low water and energy costs.

By contrast, the matrix hydrogen concentration distribution in Figure 7 reveals a different behavior. Concentrations are localized and attenuated, with values significantly lower than those observed in fractures. The patchy distribution reflects the limited contribution of the matrix to overall recovery, a consequence of lower permeability and slower diffusion processes. This observation aligns with the model's prediction that the matrix contributes minimally to total recovery, underscoring the need for enhancement strategies such as chemical stimulation to increase reactivity or thermal stimulation to accelerate diffusion and desorption. The figure also highlights the heterogeneity of reservoir performance, where matrix zones act more as secondary storage rather than primary flow pathways.

Taken together, the two figures validate the DPDP representation by illustrating the duality of reservoir behavior: fractures act as high-efficiency flow channels. At the same time, the matrix functions as a low-efficiency reservoir. This duality explains the efficiency trade-offs identified in the system-wide benchmarks, where fracture-driven recovery achieves specific energy consumption of 3.4 MJ/kg H_2 and specific water consumption of 0.02 m^3/kg H_2, an order of magnitude lower than conventional hydrogen production methods. At the same time, the limited matrix contribution points to opportunities for optimization through stimulation design and reservoir characterization. These results emphasize that while fracture systems provide the cornerstone of geologic hydrogen recovery, unlocking the potential of the matrix remains a critical frontier for future research and development.

CONCLUSION

This study presents an integrated modeling framework for estimating resource usage associated with geologic hydrogen extraction via hydraulic fracturing. By adapting published shale gas production results for benchmarking and applying the framework to a multi-well hydrogen development scenario, the model demonstrates its capability to simulate fracture-controlled production dynamics and associated resource utilization under representative subsurface conditions. The results highlight the dominant role of fracture networks in controlling hydrogen recovery and illustrate how production behavior, water use, and energy inputs evolve during reservoir operation.

A key component of the framework is the phenomenological reaction-extent formulation used to represent hydrogen-generating reactions. Although simplified relative to detailed geochemical models, this approach provides a practical means of exploring hydrogen generation and production efficiency in the absence of well-constrained field-scale kinetic data. Under the simulated multi-well scenario, the framework produced indicative performance metrics including cumulative hydrogen production of approximately 1.13 million kg, a water utilization efficiency of about 57 kg H_2/m^3, and an operational energy intensity of roughly 3.40 MJ/kg H_2, corresponding to an energy efficiency of 0.29 kg H_2/MJ. These values represent model-based estimates under the assumed conditions and illustrate the type of system-level performance indicators that the framework can generate.

The framework is intended as an exploratory tool for assessing production dynamics and resource requirements under data-limited conditions rather than as a fully validated predictive model. The benchmarking exercise against published shale gas results primarily evaluates the framework's ability to reproduce production decline behavior, while other components, including reactive transport processes and hydrogen generation kinetics, remain subject to uncertainty due to the limited availability of field-scale geologic hydrogen datasets.

Despite these limitations, the framework demonstrates how fracture-controlled production behavior, simplified reaction modeling, and resource accounting can be integrated within a single modeling structure. This integration provides a basis for evaluating water–energy–hydrogen trade-offs and exploring operational scenarios relevant to geologic hydrogen development. As experimental and field data become available, the framework can be refined through improved parameterization, sensitivity analysis, and calibration to support more detailed technical, environmental, and economic assessments of geologic hydrogen extraction.

ACKNOWLEDGEMENTS

The authors gratefully acknowledge the financial support provided by the National Research Foundation (NRF) of South Africa and the Faculty of Engineering and the Built Environment at the University of the Witwatersrand (Wits). Their funding and support made this research possible.

AUTHOR IDENTIFIERS

Author ORCIDs:
Kaitano C: 0000-0003-0303-9608
Majozi T: 0000-0003-0864-2393

REFERENCES

1. Boafo J, Dotsey S, Spencer R. Energy transition diplomacy: the eu’s pursuit of africa's critical minerals for renewable energy at whose expense?. Energy Research & Social Science 127:104213 (2025). https://doi.org/10.1016/j.erss.2025.104213
2. Dawood F, Anda M, Shafiullah GM. Hydrogen production for energy: an overview. International Journal of Hydrogen Energy 45:3847-3869 (2020). https://doi.org/10.1016/j.ijhydene.2019.12.059
3. Osman AI, Mehta N, Elgarahy AM, Hefny M, Al-Hinai A, Al-Muhtaseb AH, Rooney DW. Correction to: hydrogen production, storage, utilisation and environmental impacts: a review. Environ Chem Lett 20:2213-2213 (2022).

https://doi.org/10.1007/s10311-022-01432-x
4. Hasiuk F, Conley DM. EXPLORING GEOLOGIC HYDROGEN : A NEW FRONTIER FOR AFFORDABLE, RELIABLE ENERGY SECURITY. 2025.
5. Abdelghany MB, Shafiqurrahman A, Al-Durra A, Mohamed M, Hu J, Vaccaro A, Gao F, El Moursi MS. Hydrogen energy systems for decarbonizing smart cities and industrial applications: a review. Renewable and Sustainable Energy Reviews 226:116370 (2026). https://doi.org/10.1016/j.rser.2025.116370
6. Zgonnik V. The occurrence and geoscience of natural hydrogen: a comprehensive review. Earth-Science Reviews 203:103140 (2020). https://doi.org/10.1016/j.earscirev.2020.103140
7. Maiga O, Deville E, Laval J, Prinzhofer A, Diallo AB. Trapping processes of large volumes of natural hydrogen in the subsurface: the emblematic case of the bourakebougou H2 field in mali. International Journal of Hydrogen Energy 50:640-647 (2024). https://doi.org/10.1016/j.ijhydene.2023.10.131
8. Prinzhofer A, Moretti I, Françolin J, Pacheco C, D'Agostino A, Werly J, Rupin F. Natural hydrogen continuous emission from sedimentary basins: the example of a brazilian h2-emitting structure. International Journal of Hydrogen Energy 44:5676-5685 (2019). https://doi.org/10.1016/j.ijhydene.2019.01.119
9. Osselin F, Soulaine C, Fauguerolles C, Gaucher EC, Scaillet B, Pichavant M. Orange hydrogen is the new green. Nat. Geosci. 15:765-769 (2022). https://doi.org/10.1038/s41561-022-01043-9
10. Templeton AS, Ellison ET, Kelemen PB, Leong J, Boyd ES, Colman DR, Matter JM. Low-temperature hydrogen production and consumption in partially-hydrated peridotites in oman: implications for stimulated geological hydrogen production. Front. Geochem. 2: (2024). https://doi.org/10.3389/fgeoc.2024.1366268
11. Egert R, Neupane G, Jin W. On the viability of stimulated hydrogen generation from iron-rich formations. Geoenergy Science and Engineering 256:214130 (2026). https://doi.org/10.1016/j.geoen.2025.214130
12. Awosiji V, Graham S, Mukerji T. The concept of a blind hydrogen system. International Journal of Hydrogen Energy 158:150492 (2025). https://doi.org/10.1016/j.ijhydene.2025.150492
13. Angelina NM, Isah A, Samouei H, Okoroafor ER. Can stimulated geological hydrogen generation systems be circular?. SPE Annual Technical Conference and Exhibition : (2025). https://doi.org/10.2118/227940-ms
14. Mao S, Yu S, Xu J, Chen H, Zhao W, Blunt MJ, Kang Q, Gross M, Chen B, Van Wijk J, Yuan Q, Gao K, Kazi SR, Mehana M. Geologic hydrogen: a review of resource potential, subsurface dynamics, exploration, production, transportation, and research opportunities. Energy Environ. Sci. 18:9991-10035 (2025). https://doi.org/10.1039/d5ee02910d
15. Jiang L, Ma Y, Wu J, Liu J, Liu T. Modeling production decline for fractured wells with non-uniform fracture properties: a semi-analytical approach based on double-segment fracture model. Processes 13:3627 (2025). https://doi.org/10.3390/pr13113627
16. Zhao G, Yao Y, Wang L, Adenutsi CD, Feng D, Wu W. Optimization design of horizontal well fracture stage placement in shale gas reservoirs based on an efficient variable-fidelity surrogate model and intelligent algorithm. Energy Reports 8:3589-3599 (2022). https://doi.org/10.1016/j.egyr.2022.02.228